Fluid Phase Equilibria 407 (2016) 197.e1–197.e10

Contents lists available at ScienceDirect

Fluid Phase Equilibria

journal homepage: www.elsevier.com/locate/fluid

Molecular dynamics simulation for self-diffusion coefficients of ginger bioactive compounds in subcritical water with and without ethanol

Nor Ilia Anisa[a,b], Noor Azian Morad[a,b,*], Yoshio Iwai[c], Mohd Halim Shah Ismail[d]

[a] Malaysia–Japan International Institute of Technology, Universiti Teknologi Malaysia, 54100 Kuala Lumpur, Malaysia
[b] Center of Lipids Engineering and Applied Research (CLEAR iKohza), Universiti Teknologi Malaysia, 54100 Kuala Lumpur, Malaysia
[c] Department of Chemical Engineering, Kyushu University, 744 Motooka, Nishi-ku, Fukuoka 819-0395, Japan
[d] Department of Chemical and Environmental Engineering, Universiti Putra Malaysia, 43300 Serdang, Malaysia

ARTICLE INFO

Article history:
Received 13 March 2015
Received in revised form 9 June 2015
Accepted 13 June 2015
Available online 23 June 2015

Keywords:
Extraction process
Subcritical water
Self-diffusion coefficient
Ginger bioactive compound
Entrainer
Ethanol

ABSTRACT

Molecular dynamics simulation was used to calculate the self-diffusion coefficients of ginger bioactive compounds (6-gingerol and 6-shogaol) in subcritical water with the presence of ethanol as an entrainer (0–10 mol%) at temperatures from 373.15 to 453.15 K. The all-atom optimised-potentials (OPLS/AA) were employed for the ginger bioactive compounds and ethanol. The extended simple point charge (SPC/E) model was adopted for water molecules. The self-diffusion coefficients increase from 1.00×10^{-9} to 2.70×10^{-9} m^2/s with increasing temperature from 353.15 to 453.15 K. The self-diffusion coefficients also increase from 1.71×10^{-9} to 3.00×10^{-9} m^2/s with increasing percentage of ethanol from 0 to 10 mol% at 413.15 K. The radial distribution functions between the ginger bioactive compounds and subcritical water (solvent) illustrate a weak interaction between the ginger bioactive compounds and solvent. The interaction increases with addition of ethanol as entrainer.

© 2015 Elsevier B.V. All rights reserved.

1. Introduction

The extraction of bioactive compounds from natural plants receive a great attention from researchers and industries due to market demands [1]. Solvent extraction is one of the conventional techniques to extract the bioactive compounds. However, this conventional technique which requires extended extraction duration and high production cost due to solvent recovery causes the researchers to use other alternative techniques. Subcritical water extraction is an environment friendly technique of utilizing water in its liquid state under pressurized condition at a temperature below the critical point. The subcritical water extraction is known as hot compressed water extraction as the process operates at elevated temperature (above boiling point of water at 373.15 K and below its critical value at 647.65 K and 22.09 MPa). The key point of operating at such elevated temperature is due to the decreasing polarity of the solvent hence improving suitability to extract non-polar compounds. Previous studies also introduce entrainer to subcritical water extraction in order to tune to the desired polarity of the solvent [2,3]. Ethanol is commonly used as an entrainer since it has low toxicity. Thus the contamination of ethanol in foods could be neglected. The extraction from natural plants using this technique has been applied on ginger [4], jabuticaba skin [5], and barberry fruits [6]. Despite the increasing demands in bioactive compounds, the application of hot compressed water technique for natural extract is still scarce.

The phenomena of extraction are important for optimising the recovery, which is commonly described through a mathematical study [7]. The phenomena of extracting the solute in solid matrix to bulk solvent involve mass transfer through solid–liquid interface. The transportation occurs due to the concentration gradient that is primarily controlled by effective diffusion coefficient, D_{eff} [8]. The D_{eff} is determined by taking into account the porosity, ε and tortuosity, τ of solid matrix [7]. In determining $D_{eff,}$ the diffusion coefficient, D is firstly identified. The diffusion coefficient, D describes the movement of solute from the outer surface of solid matrix into the bulk of solvent, i.e. the movement of solute in solvent. In a complex matrix such as plant matrix, the effective diffusion coefficient, D_{eff} is by the following equation [9]:

$$D_{eff} = \frac{\varepsilon}{\tau} D \quad (1)$$

Abbreviations: OPLS/AA, all-atom optimised-potentials; SPC/E, extended simple point charge; MD, molecular dynamics; NPT, isothermal–isobaric ensemble; NVT, canonical ensemble; MSD, mean squared displacement; SD, standard deviation; ANOVA, analysis of variance; RDF, radial distribution function.

* Corresponding author at: Center of Lipids Engineering and Applied Research (CLEAR iKohza), Universiti Teknologi Malaysia, 54100 Kuala Lumpur, Malaysia. Fax: +60 3 26154317.
E-mail address: azian.morad@gmail.com (N.A. Morad).

http://dx.doi.org/10.1016/j.fluid.2015.06.018
0378-3812/© 2015 Elsevier B.V. All rights reserved.

Nomenclature

Roman letters

V_1,V_2,V_3	Coefficients in the Fourier series (parameter in Eq. id=6#(2))
f_1, f_2, f_3	Phase angles (parameter in Eq.id=6#(2))
q	Charge, ^{-}e (parameter in Eq.id=6#(3))
D	Self-diffusion coefficient, (m^2/s)
D_{eff}	Effective diffusion coefficient, (m^2/s)
N	Number of time series
r	Position vector of molecule, (Å)
$g(r)$	Radial distribution function

Greek letters

φ_i	Dihedral angle
ε	Energy parameter, (kJ/mol) (parameter in Eq.id=6#(3))
σ	Size parameter, (Å) (parameter in Eq.id=6#(3))
$\rho(r)$	Local number density, (m^{-3})
ρ	Bulk number density, (m^{-3})

Subscripts

i, j	Sites
a, b	Molecules

As claimed by Takeuchi [8], the range of diffusion coefficients is 10^{-9}–10^{-10} m^2/s for food solutes in different types of solvent. Balachandran et al. [10] determined the diffusion coefficient of 6-gingerol in supercritical carbon dioxide as 7.20×10^{-9} m^2/s using an equation and D_{eff} by fitting concentration gradient against time. The calculated values of diffusion coefficients for gallic acid, catechin and procyanidin from grape pomace at 313.15 K are 2.22×10^{-9}, 1.42×10^{-9} and 0.79×10^{-9} m^2/s, respectively [11]. Srinivas et al. [12] found the determination of diffusion coefficients is difficult at temperatures higher than 352.15 K but still the diffusion coefficients can be predicted by Stokes–Einstein model.

A few techniques such as experimental, molecular dynamics simulation, empirical or theoretical approaches are used to determine the diffusion coefficients [13]. The experimental data such as by using Taylor dispersion can be found in the literature [13–17]. The literature data are limited to lower temperatures and mostly for smaller compounds only. The empirical or theoretical method often fails to predict reliable values of the diffusion coefficients especially when it dealing with highly polar or involving hydrogen-bonding [13].

Molecular dynamics (MD) simulation can be used to calculate the self-diffusion coefficients of solutes in solvents [18] and is a powerful tool with unique resolution down to Angstrom scale with picosecond calculation time [19]. However the application of MD simulation for food based solutes in water as solvent is limited at ambient temperature and to our knowledge it has never been applied to bioactive compounds at high temperature. Delgado [20] studied the effects of temperature on the self-diffusion coefficients of organic compounds such as 2-naphthol, benzoic acid, salicylic acid, camphor, and cinnamic acid in water below its boiling point using MD simulation. In another study of using MD simulation, Fioroni et al. [21] investigated the solvation phenomena of a tetrapeptide in water at ambient temperature. Paul and Patey [22] investigated the self-diffusion coefficients for urea in water also at ambient temperature and pressure. The other papers using MD simulation investigated the self-diffusion coefficients of methane in water at elevated temperatures from 296.15 to 650.15 K [23] and phenol in water in the range of 298.15–773.17 K [17].

In this work, MD simulation is employed to calculate the self-diffusion coefficients of the most abundant bioactive compounds in ginger extract; 6-gingerol and 6-shogaol in subcritical water with and without ethanol. The radial distribution functions which describe the interaction between the bioactive compounds and solvent are also studied. To the best of our knowledge, there are no previous data for the self-diffusion coefficients and radial distribution functions of larger compound + water and compound + water/ethanol at subcritical conditions. Thus, from this paper, the data can be expected to contribute to design the extraction parameters, especially when the entrainer (ethanol) is added in water at subcritical conditions.

2. Computational details

2.1. Intermolecular potential

The all-atom optimised-potential liquid simulation (OPLS/AA) has been used for describing the intermolecular potentials of phenol, ethanol and the ginger bioactive compounds (6-gingerol and 6-shogaol) since this force field is suitable for the organic and biomolecular systems [24]. The united-atom optimised-potential liquid simulation (OPLS/UA) was employed for CH_3 of anisole group in ginger bioactive compounds. This is because of the charge for CH_3 of anisole group are different from that for CH_3 of paraffins, and the charges of CH_3 of anisole group for OPLS/AA are not available in the literature. The SPC/E model [25] was adopted for water molecules.

The torsional energies were calculated by the following equation [24]:

$$E_{\text{torsion}} = \sum_i \frac{V_{1,i}}{2}[1 + \cos(\varphi_i + f_{1,i})] + \frac{V_{2,i}}{2}[1 - \cos(2\varphi_i + f_{2,i})] + \frac{V_{3,i}}{2}[1 + \cos(3\varphi_i + f_{3,i})] \quad (2)$$

where ϕ_i is the dihedral angle, V_1, V_2 and V_3 are the coefficients in the Fourier series and f_1, f_2 and f_3 are the phase angles. The bond lengths and angles in the molecules were fixed to the equilibrium values to reduce the computation time.

The non-bonded interactions were explained by a combination of Coulomb with Lennard–Jones as follows [24]:

$$E_{ab} = \sum_i^{\text{on}a} \sum_j^{\text{on}b} \left[\frac{q_i q_j e^2}{r_{ij}} + 4\varepsilon_{ij} \left(\frac{\sigma_{ij}^{12}}{r_{ij}^{12}} - \frac{\sigma_{ij}^{6}}{r_{ij}^{6}} \right) \right] f_{ij} \quad (3)$$

where E_{ab} is the interaction energy between molecules a and b for sites i and j, respectively. The q, ε, σ and r are the charge, the energy parameter, the size parameter, and the site distance, respectively. Modification of Eq. (1) has been made by Jorgensen et al. [24] to authorize the usage of the same parameters for inter- and intramolecular interaction. Thus, the scaling factors f_{ij} for all cases is 1.0, otherwise $f_{ij} = 0.5$ for 1,4-interaction [24]. Lorentz–Berthelot (LB) mixing rules were applied in determining the mixing pair of sites [26]:

$$\sigma_{ij} = \frac{\sigma_i + \sigma_j}{2} \quad (4)$$

$$\varepsilon_{ij} = \sqrt{\varepsilon_i \varepsilon_j} \quad (5)$$

The structure of ginger bioactive compound (6-gingerol) is shown in Fig. 1. The parameters and the charges are listed in Table 1.

2.2. Operating conditions

Molecular dynamics simulation was performed by the software SCIGRESS ME Compact 2.0 (Fujitsu Ltd., Japan). The simulation cell

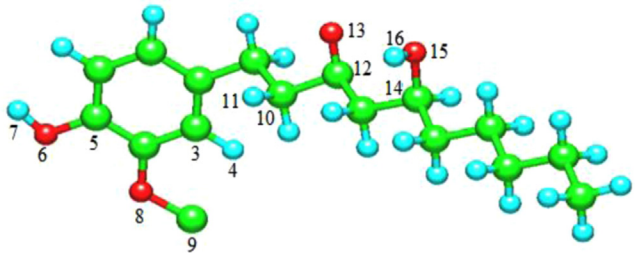

Fig. 1. Structure of ginger bioactive compound (6-gingerol). 6-Shogaol obtains similar structure except hydroxyl (atoms of number 15 and 16) is replaced by hydrogen and double bond present between carbon 4 and 5 in the decyl chain.

Table 1
Potential parameters and charges.

Molecule	Symbol	Atom	σ (Å)	ε (kJ/mol)	$q(e)$	Ref
Water	1	O	3.166	0.481	−0.848	[25]
	2	H	0.000	0.000	+0.424	
Ginger bioactive compounds, phenol and ethanol	3	C_{ar}	3.550	0.293	−0.115	[24]
	4	H_{ar}	2.420	0.126	+0.115	
	5	C_a	3.550	2.929	+0.150	
	6	O_a	3.070	0.711	−0.585	
	7	H_a	0.000	0.000	+0.435	
	8	O_b	3.000	0.711	−0.385	
	9	C_b	3.800	0.711	+0.250	
	10	C_c	3.500	0.276	−0.120	
	11	H_b	2.500	0.126	+0.060	
	12	C_d	3.750	0.439	+0.470	
	13	O_c	3.550	0.293	−0.470	
	14	C_e	3.500	0.276	+0.265	
	15	O_d	3.120	0.711	−0.683	
	16	H_c	0.000	0.000	+0.418	

Notes: (C_{ar}), C in aromatic ring; (H_{ar}), H in aromatic ring; (C_a), C in aromatic ring connected to OH; (O_a), O connected to C_a; (H_a), H connected to O_a; (O_b), O connected to CH_3 and C_{ar}; (C_b), CH_3 of anisole connected to O_b; (C_c), C in alkane chain; (H_b), H in alkane chain; (C_d), C in ketone; (O_c), O in ketone; (C_d), C in alkane chain connected to OH; (O_d), O in alcohol connected to C_e; (H_c), H in alcohol connected to O_d.

was generated at 10.23 MPa (1500 psi) with temperatures range from 353.15 to 453.15 K. Nose method [27] and Parrinello–Rahman method [28] were adopted for temperature and pressure control, respectively. The isokinetic equations of motions were integrated using the fifth-order Gear algorithm with time step of 1 fs. The Ewald sum [29] method was applied for the coulomb potentials in the periodic boundary. The cut-off distance for Lennard–Jones potentials was set to 12 Å which was close to half of the cell length. The calculation was performed with NPT ensemble for 20 ps to calculate the equilibrium density. After 20 ps, the initial conformation is not significant since it changed quickly during the simulation. Then NVT ensemble was adopted for 700 ps to calculate the self-diffusion coefficients and radial distribution functions at each condition. The procedure was repeated for the entrainer effect using ethanol from 0 to 10 mol% at 413.15 K.

The self-diffusion coefficients, D of phenol in subcritical water were first calculated by molecular dynamics (MD) simulation to compare with the literature values [15] and verify the methods adopted in this work. To the knowledge of the authors, the paper of Plugatyr and Svishchev [17] is the only reference that determined the D in subcritical water using MD simulation. There are a few studies that also determined the D of compounds in water, but at a lower temperature [20,30].

2.3. Calculation of self-diffusion coefficients

The Einstein relation was applied to determine the self-diffusion coefficients through the mean squared displacement (MSD) [31]:

$$D = \frac{1}{6N}\lim_{t\to\infty}\frac{\mathrm{d}}{\mathrm{d}t}\left\langle |r_i(t) - r_i(0)|^2 \right\rangle \quad (6)$$

where $r_i(t)$ is the position vector of centre of solute i at time t, N is the number of time series and the angular bracket, <...> denotes the ensemble average. The sub-average of self-diffusion coefficients was evaluated with the time length of 11.01 ps, the shift time of 10 fs, and the number of time series of 4722. The procedure was performed until 700 ps for each solute to get ten sub-average of the self-diffusion coefficients. The self-diffusion coefficients and the standard deviation of each solute are obtained with the ten sub-average of diffusivities.

2.4. Calculation of the radial distribution functions (RDFs)

The RDFs provide quantitative information on the interaction of each site with solvent at the molecular level [32]. The radial distribution function, $g(r)$ is defined as follows [33]:

$$g(r) = \frac{\rho(r)}{\rho} \quad (7)$$

where $\rho(r)$ is the local number density, and ρ is the bulk number density.

2.5. Statistical analysis

All determinations were carried out with standard deviation and data expressed as mean ± SD values. The level of significance was set at $p < 0.05$ and evaluated by a one-way analysis of variance (ANOVA) [34], using the Microsoft Excel (Microsoft Professional Plus, version 2010, Microsoft Corporation).

3. Results and discussion

3.1. Validation of self-diffusion coefficients using molecular dynamic (MD) simulation

Table 2 shows the comparison of the calculated results of the self-diffusion coefficients of phenol in water at two temperatures, 373.15 and 423.15 K by Plugatyr and Svishchev [17] and this study. The system size was 503 water molecules and 1 phenol molecule which is the same as in the literature [17]. The SPC/E potential was adopted by Plugatyr and Svishchev [17]. However, they did not mention the potential parameters of phenol in the literature. The results of this work are almost the same as those of Plugatyr and

Table 2
Comparison of experimental data [17] and MD simulations for self-diffusion coefficients of phenol in water at 25.0 MPa.

Temperature (K)	Self-diffusion coefficient, $D \times 10^9$ (m^2/s)			[a]Deviation (%)
	MD simulation [17]	MD simulation in this work	Experimental data [17]	
373.15	2.61	2.55 ± 0.02	3.90	−35
423.15	4.72	4.25 ± 0.03	6.64	−36

[a] Compared between MD simulation results in this work with experimental data.

Svishchev [17] at both temperatures. Table 2 shows the comparison of the self-diffusion coefficients of phenol in water at 373.15 and 413.15 K between the experimental data [17] and the calculated results by MD in this work. The deviations at both temperatures are about 35%. Shvab and Sadus [23] stated that the deviation values of diffusivities using MD simulation is about 35% when compared with the experimental data at higher temperatures. Yui et al. [30] measured the self-diffusion coefficients of phenol in water, but the operating temperature was lower than the subcritical conditions. Still the increment of the self-diffusion coefficients with temperature is found in their paper. In agreement with the findings of this work, Wang et al. [35] found the self-diffusion coefficients calculated by MD simulation were lower than those of the experimental data at temperatures higher than 340.0 K for most compounds they studied.

3.2. Factors affecting self-diffusion coefficients

The system size was firstly investigated. The simulated self-diffusion coefficients of 6-gingerol at 413.15 K and 10.34 MPa were 1.85×10^{-9} and 1.77×10^{-9} m^2/s for 1000 and 503 water molecules, respectively. Since the number of water molecules has insignificant effect on the result of the self-diffusion coefficients ($p > 0.05$), then, the number of water molecules was fixed to 503 with one molecule of solute (either 6-gingerol or 6-shogaol) to minimize the simulation time.

The self-diffusion coefficients depend on a number of factors such as temperature, solvent properties and solute itself [36]. The effect of temperature on the self-diffusion coefficients of ginger bioactive compounds, 6-gingerol and 6-shogaol in subcritical water is shown in Fig. 2. Both ginger bioactive compound demonstrates have a similar trend on self-diffusion coefficients at the lower temperature studied in the range of 353.15 to 393.15 K, respectively. However, at higher temperatures the self-diffusion coefficients of 6-shogaol are slightly higher than those of 6-gingerol. The self-diffusion coefficients of 6-gingerol increase from 1.14×10^{-9} to 2.45×10^{-9} m^2/s with increasing temperature from 353.15 to 453.15 K. 6-Shogaol demonstrates similar trends as 6-gingerol where the self-diffusion coefficients increase from 1.18×10^{-9} to 2.66×10^{-9} m^2/s between 353.15 and 453.15 K. The overall trends show the self-diffusion coefficients increases proportionally with temperature ($p < 0.05$), due to the increasing of kinetic energy and decreasing density of water as the temperature increases. Confirming the findings of this work, Poudyal and Adhikari [37] also found the temperature dependence of the self-diffusion coefficients of carbon monoxide in water using MD simulation. The self-diffusion coefficients increase from 2.11×10^{-9} to 4.48×10^{-9} m^2/s from 293.15 to 333.15 K. The self-diffusion coefficients of methane in water increase from 2.00×10^{-9} to 4.00×10^{-9} m^2/s as temperature increasing from 300.15 to 350.15 K [23]. As compared to 6-gingerol, the self-diffusion coefficients of methane in water at the same temperatures are higher since methane is much smaller than the ginger bioactive compounds.

The temperature dependency of the self-diffusion coefficients can be described by Arrhenius equation. The activation energy which gives information on the interaction between solute and solvent is related to the self-diffusion coefficients through Arrhenius equation. The relationship of the self-diffusion coefficients, activation energy and temperature is expressed by Arrhenius equation as follows:

$$\ln D = \ln D_0 - \frac{E_a}{RT} \tag{8}$$

where D and D_0 are the self-diffusion coefficients at given temperature and the initial self-diffusion coefficient, respectively, E_a is the activation energy, and R is the universal gas constant (8.314 kJ/mol K). By plotting ln D versus $1/T$, the activation energies and initial diffusivities of the ginger bioactive compounds were determined. The linear correlations of ln D versus $1/T$ are obtained as shown in Fig. 3. The activation energies for 6-gingerol and 6-shogaol are 9.9 and 12.3 kJ/mol, respectively. The activation energy of 6-gingerol is lower than that of 6-shogaol because it has higher molecular weight (294.39). The activation energy of *trans*-resveratrol is 29.0 kJ/mol [38], which is higher than those of 6-gingerol and 6-shogaol since it has lower molecular weight of 228.2. The correlation of self-diffusion coefficients and molecular weights has been postulated by Martins et al. [39] in their paper.

The discrepancy of the activation energies between 6-gingerol and 6-shogaol could be explained by the properties of the compounds itself. The higher activation energy calculated for a particular compound indicates the lower reaction rate of that compound [40]. 6-Gingerol has hydroxyl group that should further enhance the interaction of its compound with subcritical water. But, as mentioned earlier subcritical water at higher temperature changes its properties to become slightly polar or nonpolar thus the expected enhanced interaction between water and 6-gingerol

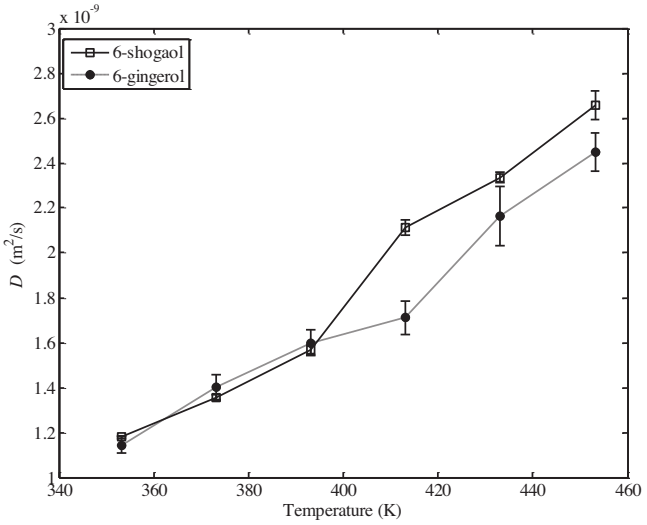

Fig. 2. Self-diffusion coefficients of ginger bioactive compounds as a function of temperature in subcritical water.

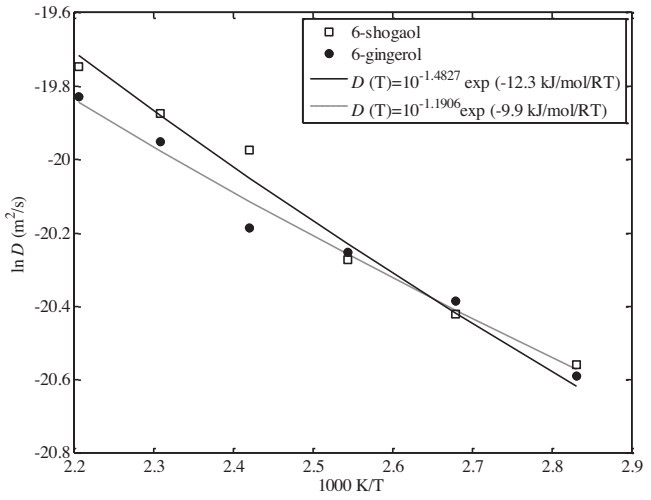

Fig. 3. Arrhenius relationship between self-diffusion coefficients and temperatures for ginger bioactive compounds in subcritical water.

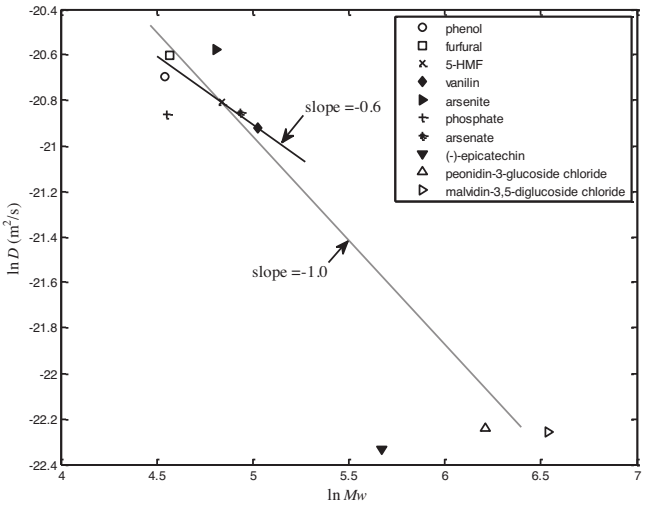

Fig. 4. Correlation of self-diffusion coefficients with molecular weight (Mw) for various solutes in water at 298.15 K. The diffusivities of solutes are cited as follows; phenol [17], furfural [30], 5-HMF [30], vanillin [30], arsenite [45], phosphate [45], arsenate [46], (-)-epicatechin [10], peonidin-3-glucoside chloride [12], malvidin-3,5-diglucoside chlorie [12].

is not observed due to the weaken OH charges in the solvent. This findings is confirmed by Carr et al. [41] which found that compounds with fewer hydroxyl group tends to have higher yield that also results on the higher diffusion coefficients. This can be related to 6-shogaol which has lower hydroxyl group compared to 6-gingerol.

The Wilke–Chang equation is widely used to correlate the self-diffusion coefficients of solute A in solvent B. The equation is expressed by the following equation [42]:

$$D = \frac{7.4 \times 10^{-8} (\phi \mathrm{Mw_B})^{1/2} T}{\eta_B V_A^{0.6}} \tag{9}$$

where $\mathrm{Mw_B}$ is the molecular weight of water, T is the temperature, η_B is the viscosity of water, V_A is the molar volume of solute at its normal boiling temperature, and ϕ is the association factor of water ($\phi = 2.6$). The following equation can be obtained.

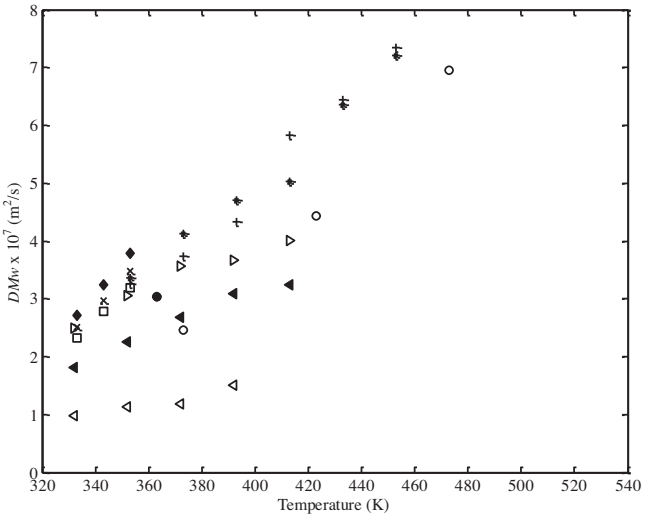

Fig. 5. Variation of experimental data of self-diffusion coefficients of the solutes in water as a function of temperatures. The data represents the solutes of (○) phenol [17], (□) furfural [30], (×) 5-HMF [30], (*) 6-gingerol, (+) 6-shogaol, (◆) vanillin [30], (◁) (-)-epicatechin [12], (◀) peonidin-3-glucoside chloride [12], (▷) malvidin-3, 5-diglucoside chloride [12], (●) caffeine [47].

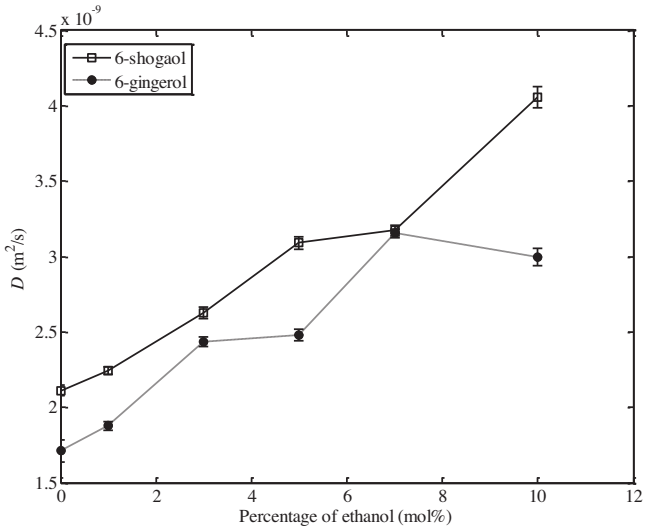

Fig. 6. Effect of percentage of ethanol on self-diffusion coefficients of ginger bioactive compounds at 413.15 K.

$$\ln D = \ln \frac{7.4 \times 10^{-8} (\phi \mathrm{Mw_B})^{1/2} T}{\eta_B} - 0.6 \ln V_A \tag{10}$$

The first term of right-hand side in Eq. (10) can be calculated from the properties of water and temperature. The densities of organic liquids are almost the same. Thus, one can assume that the molar volume of solute at its normal boiling temperature is proportional to the molecular weight of solute. From Eq. (10), ln D versus ln Mw can be explained by a straight line with slope of −0.6. Fig. 4 shows the correlation of diffusion coefficients for various solutes with molecular weights, Mw in water as solvent at 298.15 K. The Wilke–Chang equation (the slope is −0.6 which is represented by a solid line) is useful for relatively small solutes.

Over the wide range of molecular weights of solutes from 41.05 of acetonitrile to 691.03 of malvidin-3,5-diglucoside chloride, the diffusion coefficients at 298.15 K are proportional to $\mathrm{Mw}^{-1.0}$. The correlation is not the same as the empirical correlation of Wilke–Chang [42] with the slope of −0.6 (represented by a solid line). The discrepancy is due to the association of the interaction of high molecular weight compounds such as (-)-epicatechin,

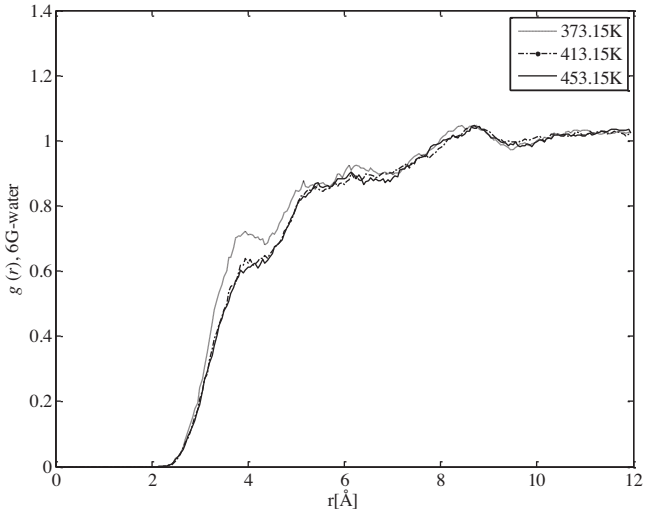

Fig. 7. Radial distribution functions between centres of mass of 6-gingerol (6G) and water.

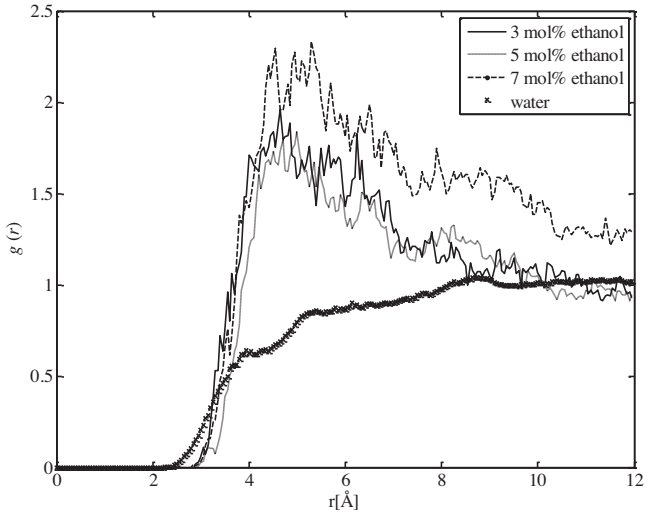

Fig. 8. Radial distribution functions between centres of mass of 6-gingerol and water, and those of 6-gingerol and ethanol at 413.15 K.

peonidin-3-glucoside chloride and malvidin-3, 5-diglucoside chloride with water. The aggregation of solutes would increase the substantial molar volumes of solvents [43]. Thus, the D of solute in water is primarily controlled by the molecular size and secondly by the interaction of solute and solvent [44].

Therefore, by multiplying the factor $Mw^{1.0}$ to D which, the trends for various solutes with temperature could be investigated as shown in Fig. 5. It also can be seen the diffusion coefficients of all solutes are close to each other since the values are the same magnitude of order at given particular temperatures. A straight line could be observed for phenol even though at higher temperature of 480.15 K because of the lower molecular weight of 94.01. In contrast, the inconsistency of DMw was illustrated for the larger molecular size compounds such as peopeonidin-3-glucoside chloride and malvidin-3,5-diglucoside chloride. The other factor that contributes to the distortion of diffusion coefficients for peopeonidin-3-glucoside chloride and malvidin-3,5-diglucoside chloride is the ionic properties of those solutes. Thus, these compounds have tendency to create small electric field in hot water [12].

Fig. 6 shows the self-diffusion coefficients of ginger bioactive compounds as a function of the percentage of ethanol from 0 to 10 mol% in subcritical water. The total number of molecules of ethanol + water in the cell were fixed to 500 molecules. The individual number of molecules, i.e. ethanol and water depend on the percentage of ethanol in the system. One molecule of the ginger bioactive compounds was added in the cell. Ethanol has been chosen as entrainer in this study since it has been identified as the best organic solvent in extracting the ginger bioactive compounds [48] and relatively safe to be use in food due to its low toxicity. From the MD simulation, the self-diffusion coefficients of both 6-gingerol and 6-shogaol increase with increasing percentage of ethanol. The self-diffusion coefficients of 6-gingerol increase from 1.71×10^{-9} to 3.00×10^{-9} m^2/s with increasing the percentage of ethanol. This is in agreement with the results by Pařez et al. [13] which indicated that the diffusion coefficients increase by the

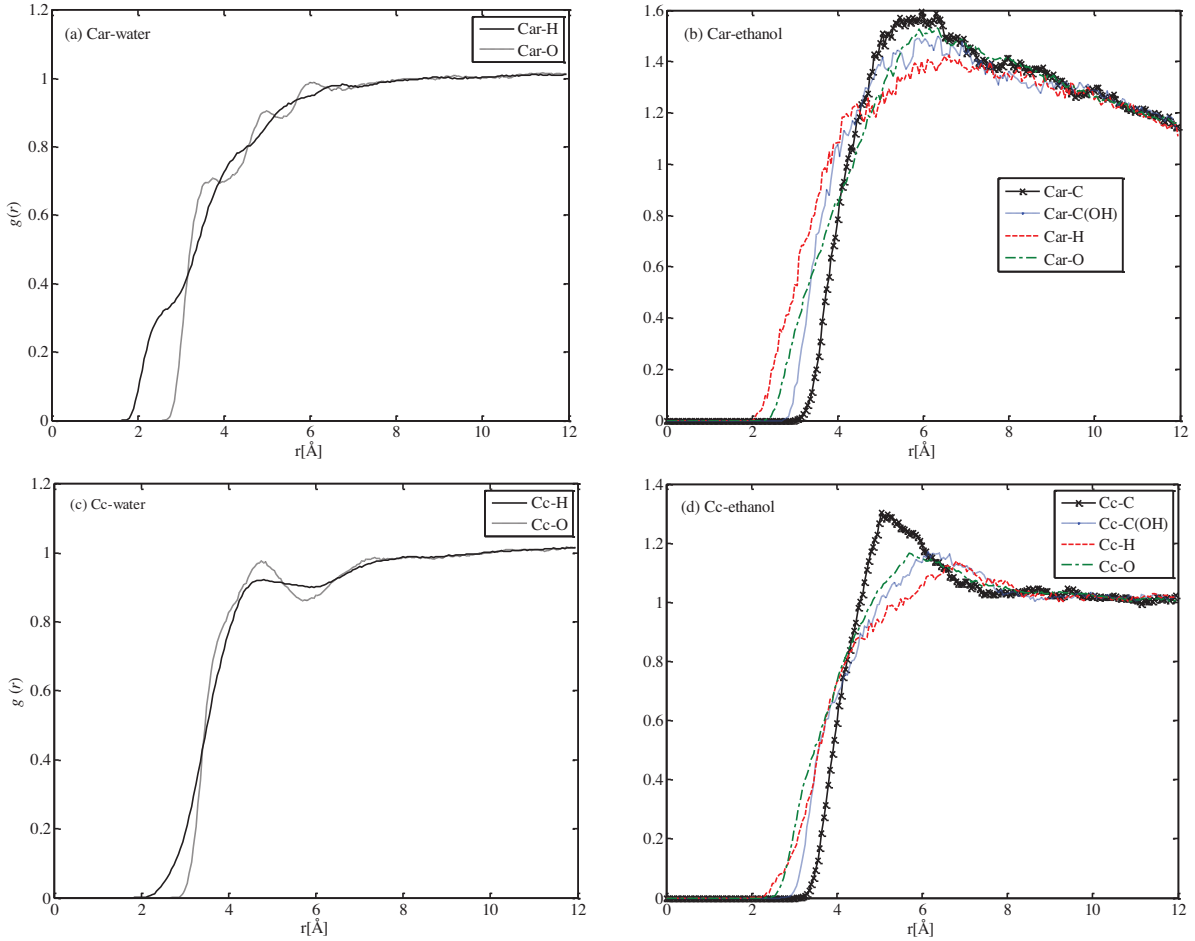

Fig. 9. Radial distribution functions between C in aromatic ring, C_{ar} and (a) water, (b) ethanol and C in alkane chain, C_c and (c) water, (d) ethanol.

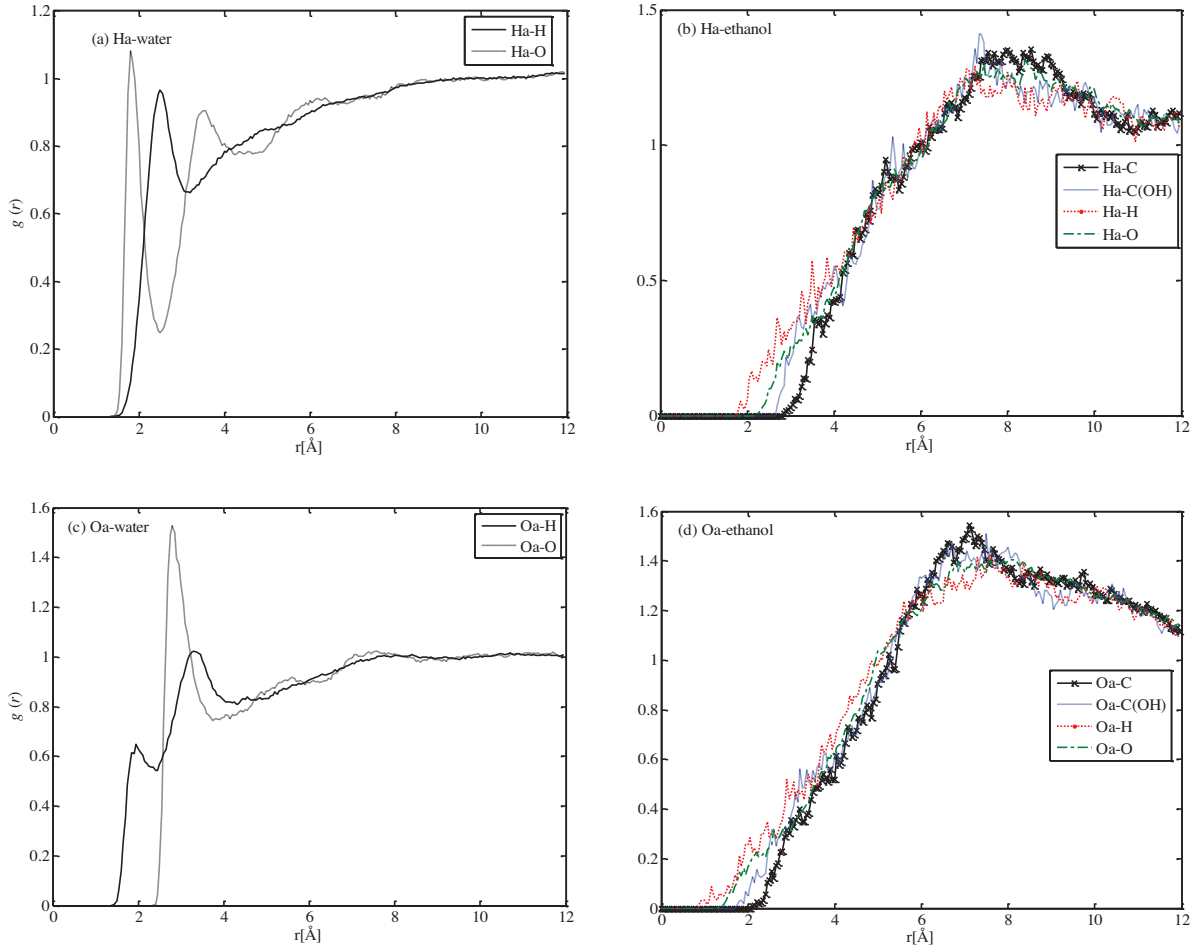

Fig. 10. Radial distribution functions between H in alcohol, H_a and (a) water, (b) ethanol and O in alcohol, O_a and (c) water, (d) ethanol.

addition of a third compound, however the diffusion coefficients are within the same order of magnitude. The increment of self-diffusion coefficients in this study is not much higher although the entrainer has been introduced. This is because of the properties of subcritical water that appropriate to extract ginger bioactive compounds. The solvent that been used in extract the compounds should conform the principle of 'like dissolve like' [4]. Thus, the results indicate that 6-gingerol is a slightly non-polar compound that requires enhancement of self-diffusion coefficients through the introduction of ethanol in subcritical water. Similar trend can be observed for 6-shagoal in which the self-diffusion coefficients increase from 2.11×10^{-9} to 4.05×10^{-9} m^2/s when ethanol is introduced in the subcritical water up to 10%. This is due to the similar structure between the two compounds. The fluctuation of self-diffusion coefficients of the ginger bioactive compounds was observed with increasing the percentage of ethanol due to the fluctuation of local densities of ethanol around the ginger active compounds. It was observed that the fluctuations of the self-diffusion coefficients for both ginger bioactive compounds are identical at 7 mol% indicating a similar solute solvent interaction.

3.3. Radial distribution function

3.3.1. Effect of temperature

In order to investigate the interaction of ginger bioactive with solvent, the radial distribution function (RDFs) were studied. Fig. 7 shows the calculated results of RDFs between the centres of mass of 6-gingerol and water at 373.15, 413.15, and 453.15 K by MD simulation. As shown in Fig. 7, the increasing temperature does not significantly affect the RDF. Only the results of 6-gingerol will be further discussed since 6-shogaol has similar trends with 6-gingerol.

3.3.2. Effect of ethanol as entrainer in subcritical water

As mentioned earlier, the self-diffusion coefficients of ginger bioactive compounds in subcritical water with ethanol are higher than those in subcritical water in the absence of ethanol. Fig. 8 shows the RDFs between centres of mass of 6-gingerol and water for binary system, and those of 6-gingerol and ethanol in aqueous solutions at 413.15 K. From the figure, the RDF between centres of mass of 6-gingerol and ethanol are shown in a broad peak and higher than unity. This indicates that the interaction of the ginger bioactive compound with the presence of ethanol in subcritical water was stronger than absence of ethanol. In contrast, no peak is observed for the RDFs between centres of mass of 6-gingerol and water. The RDFs are related with the self-diffusion coefficients which increases with the presence of ethanol. The RDFs describe the interaction of solvent that surrounded the ginger bioactive compounds. Ethanol has a weak network bonding compared to water thus the ginger bioactive compounds easy to move by addition of ethanol. The self-diffusion coefficients increase with increasing the concentrations of ethanol in water. As claimed by Carr et al. [41], the interaction of solute depends on the degree of conjugation of the aromatic rings, position of hydrogen bonding side groups around the rings and the presence of the side group in each compound. The interaction between the ginger bioactive

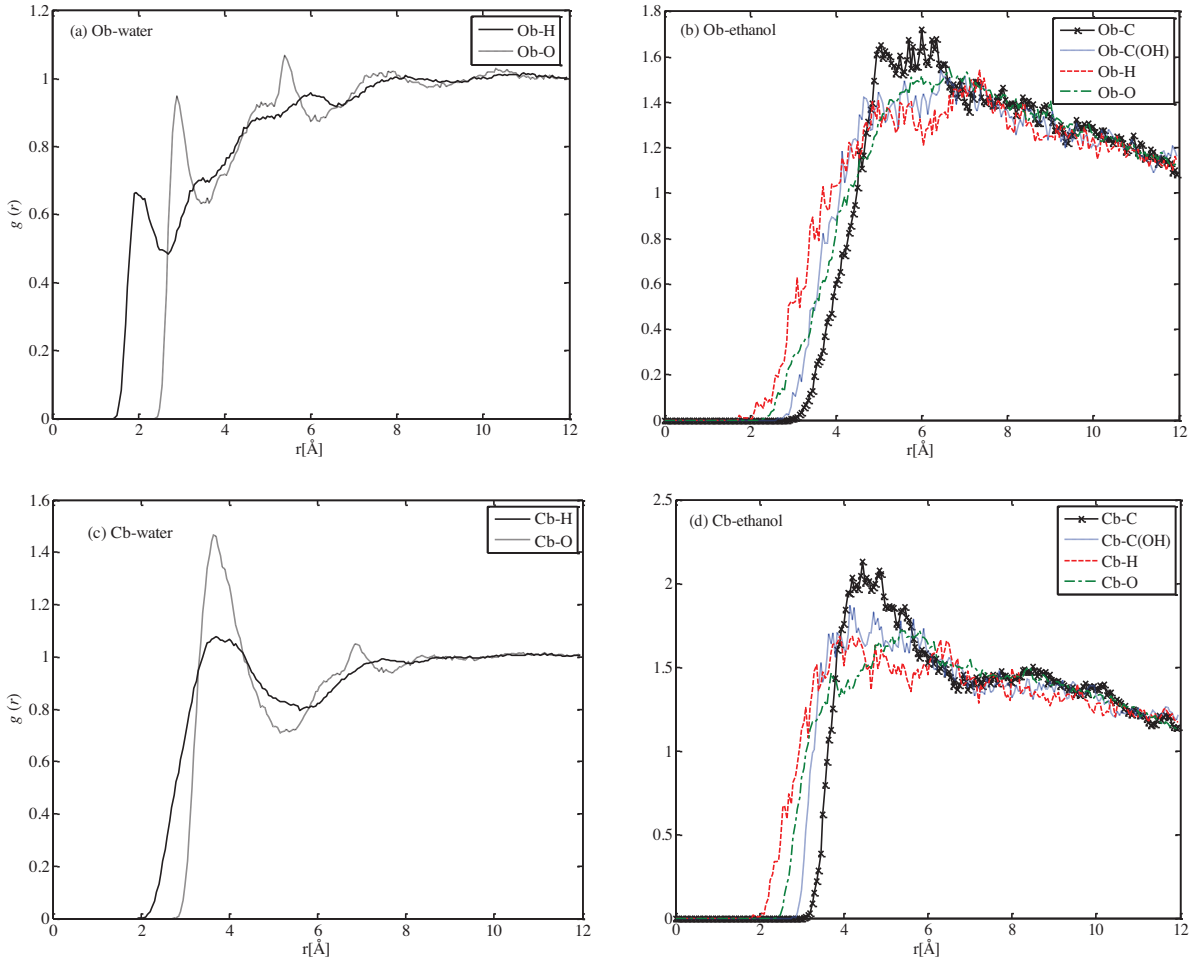

Fig. 11. Radial distribution functions between O in anisole, O_b and (a) water, (b) ethanol and C in ketone, C_b and (c) water, (d) ethanol.

compounds and solvent increases with the presence of ethanol since the ginger bioactive compounds are larger compounds with aromatic ring, alkane chain and hydroxyl group as main groups. The fluctuation of RDFs between 6-gingerol and ethanol in aqueous solutions is due to the small number of samplings. The number of ethanol molecules are much smaller than those of water molecules in the aqueous solutions.

3.3.3. Comparison of RDFs for 6-gingerol in water and ethanol

The RDFs between each site for 6-gingerol and water for binary system, and those and ethanol in 7 mol% ethanol aqueous solution are also identified at 413.15 K. The main sites discussed are carbons in aromatic and alkane chain, hydroxyl group, anisole (O—CH_3) and ketone (C=O). Fig. 9 shows the RDFs between carbon in aromatic and alkane chain for 6-gingerol and water, and those for 6-gingerol and ethanol. As shown in Fig. 9(a) and (c), the peaks of the RDFs between both the sites for 6-gingerol and water are broad, and the heights are less than unity. It means that the interactions of both the sites with water are weak. On the other hand, the interactions of both the sites with ethanol are stronger than those with water because of the peak heights of the RDFs between both the sites for 6-gingerol and ethanol are higher than unity as shown in Fig. 9(b) and (d).

The RDFs between alcohol sites (H_a and O_a) for 6-gingerol and water sites, and those for 6-gingerol and ethanol sites are shown in Fig. 10. Similar trends can be observed for the RDFs between H_a for 6-gingerol and ethanol sites and the RDFs between O_a for 6-gingerol and ethanol sites. However, the different trends for the RDFs between H_a for 6-gingerol and H for water and the RDFs between O_a for 6-gingerol and O for water. In Fig. 10(a), two peaks appear for H_a–O indicates that the hydrogen bond is found at first and second outer shell. The maximum $g(r)$ is observed at the first outer shell which is 1.1 at 1.9 Å. However, the $g(r)$ for second outer shell is less than unity thus shows that the weak interaction occurs in this outer shell. While for O_a–O, only one peak appears at $r = 2.75$ Å with $g(r)$ of 1.492 which is associated with a weak interaction with water from an outer first solvation shell interaction.

Fig. 11 shows the RDFs between anisole site for 6-gingerol and water sites, and those and ethanol sites. Similar to the previous sites, the broad peak is observed for the RDFs between anisole site for 6-gingerol and ethanol sites, and the $g(r)$ is higher than unity. Indeed, the interaction of this site with ethanol is higher than that with water due to the $g(r)$ of this site with ethanol is 1.7, and that with water is only 1.0. From Fig. 11(a), the presence of hydrogen bonds at O_b–H shows that the interaction still arises at this site although the $g(r)$ is less than unity. As shown in Fig. 11(c), the positions of the peaks for hydrogen and oxygen are almost the same for each site indicating the water molecules are located randomly around the site. Only one peak is observed from the figure which is at the outer of first hydration shell for C_b with water. The peak heights of RDFs for C_b–O and C_b–H are 1.441 and 1.057 at 3.6 Å, respectively. The carbon site in anisole has larger space and more atoms surrounding it i.e. CH_3 in this site are compared to oxygen site of anisole. Thus, the interaction of C_b is higher than O_b for both with water and ethanol.

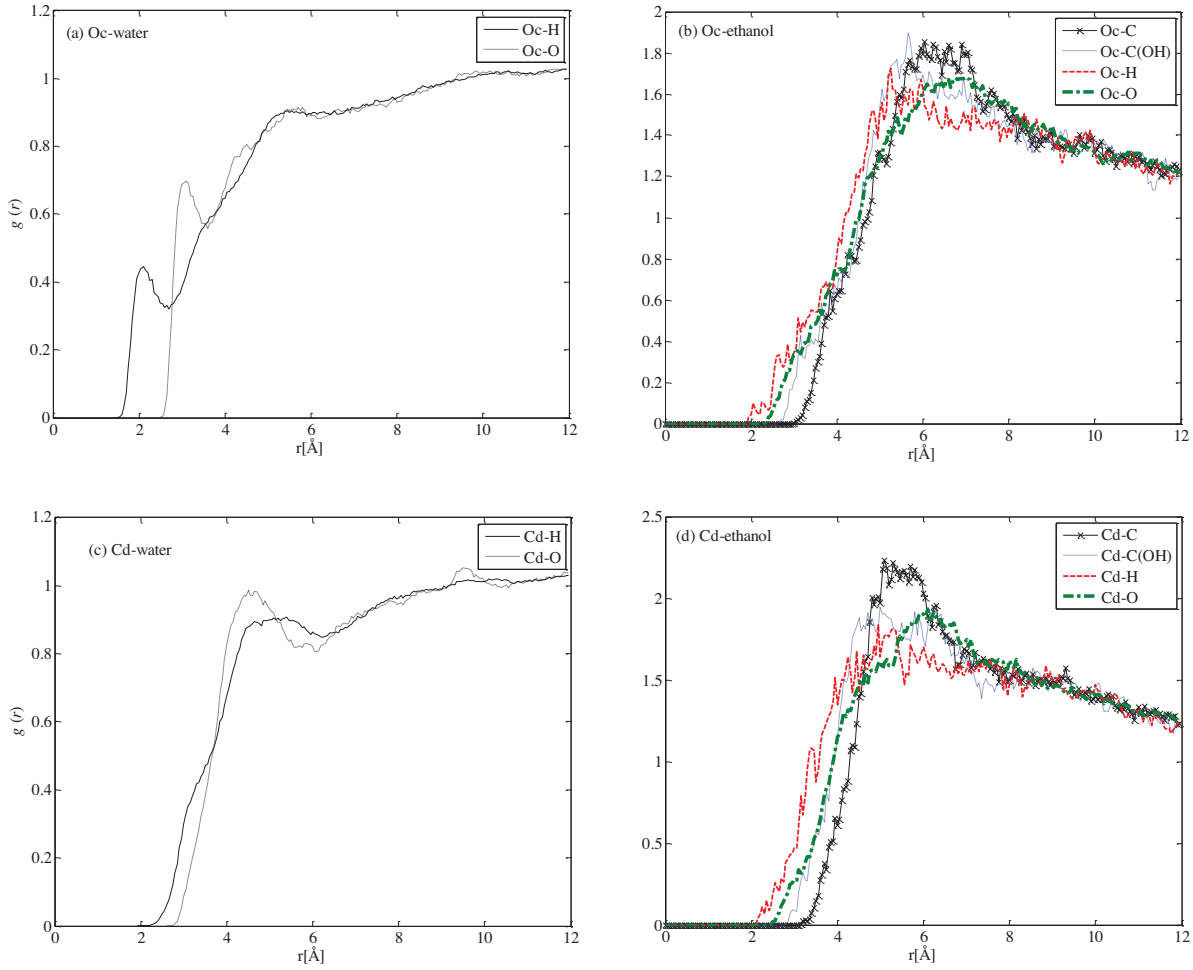

Fig. 12. Radial distribution functions between O in ketone, O_c and (a) water, (b) ethanol and C in ketone, C_d and (c) water, (d) ethanol.

Figs. 12(a) and 10(b) represent the RDFs graph of O_c–water and O_c–ethanol atomic pairs. It is clear that the interaction of this site with ethanol is higher than that with water. The peaks of g(r) for O_c–water can be observed. However, the heights are lower than unity. Water molecules cannot easy to come around the site because the alkane chain blocks the water molecules to come around to the ketone site. As shown in Fig. 12(c), the positions of the peaks for hydrogen and oxygen are almost the same for each site. Water molecules are located randomly around the site.

4. Conclusion

The self-diffusion coefficients of ginger bioactive compounds were predicted by the molecular dynamics simulation. Temperature significantly affects the self-diffusion coefficients of ginger bioactive compounds which proportionally increase with temperature about two folds from 1.14×10^{-9} m^2/s at 353.15 K to 2.66×10^{-9} m^2/s at 453.15 K. The self-diffusion coefficients of 6-gingerol and 6-shogaol in water with the presence of ethanol as entrainer indicate the enhancement of self-diffusion coefficients and is related to the percentage of ethanol presence in subcritical water. The studies of the radial distribution functions (RDFs) of 6-gingerol in water with the presence of ethanol as entrainer shows that ethanol plays an important role in changing the interaction of compounds with bulk solvent. The interaction between ginger bioactive compounds and solvent (subcritical water) increases with the presence of ethanol. Thus, the self-diffusion coefficients of the ginger bioactives increase by introducing ethanol as entrainer. This information can be further utilized to design an effective extraction process through further correlational study on effective diffusion coefficients.

Acknowledgments

This work was supported by the Malaysia–Japan International Institute of Technology (MJIIT) fellowship under Universiti Teknologi Malaysia, Kuala Lumpur, MJIIT and FRGS research funds. The author would like to acknowledge Issei Taniguchi for his assistance in this work.

Appendix A. Supplementary data

Supplementary data associated with this article can be found, in the online version, at http://dx.doi.org/10.1016/j.fluid.2015.06.018.

References

[1] S. Zhao, O.-D. Baik, Y.J. Choi, S.-M. Ki, Pretreatments for the efficient extraction of bioactive compounds from plant-based biomaterials, Crit. Rev. Food Sci. Nutr. 54 (2014) 1283–1297.
[2] F. Barros, L. Dykes, J.M. Awika, L.W. Rooney, Accelerated solvent extraction of phenolic compounds from sorghum brans, J. Cereal Sci. 58 (2013) 305–312.
[3] B. Tangkhavanich, T. Kobayashi, S. Adachi, Effects of repeated treatment on the properties of rice stem extract using subcritical water, ethanol, and their mixture, J. Ind. Eng. Chem. 20 (2014) 2610–2614.
[4] M.S. Md Sarip, N.A. Morad, N.A. Mohamad Ali, Y.A. Mohd Yusof, M.A. Che Yunus, The kinetics of extraction of the medicinal ginger bioactive compounds using hot compressed water, Sep. Purif. Technol. 124 (2014) 141–147.

[5] D.T. Santos, P.C. Veggi, M.A.A. Meireles, Optimization and economic evaluation of pressurized liquid extraction of phenolic compounds from jabuticaba skins, J. Food Eng. 108 (2012) 444–452.
[6] A. Sharifi, S.A. Mortazavi, A. Maskooki, M. Niakousari, A.H. Elhamirad, Optimization of subcritical water extraction of bioactive compounds from barberry fruit (*Berberis vulgaris*) by using response surface methodology, Int. J. Agric. Crop Sci. 6 (2013) 89–96.
[7] C. Pronyk, G. Mazza, Design and scale-up of pressurized fluid extractors for food and bioproducts, J. Food Eng. 95 (2009) 215–226.
[8] T.M. Takeuchi, C.G. Pereira, M.E.M. Braga, M.R. Marostica Jr., P.F. Leal, M.A.A. Meireles, Extracting Bioactive Compounds for Food Products: Theory and Application, CRC Press, New York, 2009.
[9] T.H. Varzakas, G.C. Leach, C.J. Israilides, D. Arapoglou, Theoretical and experimental approaches towards the determination of solute effective diffusivities in foods, Enzyme Microb. Technol. 37 (2005) 29–41.
[10] S. Balachandran, S.E. Kentish, R. Mawson, The effects of both preparation method and season on the supercritical extraction of ginger, Sep. Purif. Technol. 48 (2006) 94–105.
[11] M.S. Guerrero, J.S. Torres, M.J. Nunez, Extraction of polyphenols from white distilled grape pomace: optimization and modelling, Bioresour. Technol. 99 (2008) 1311–1318.
[12] K. Srinivas, J.W. King, L.R. Howard, J.K. Monrad, Binary diffusion coefficients of phenolic compounds in subcritical water using a chromatographic peak broadening technique, Fluid Phase Equilib. 301 (2011) 234–243.
[13] S. Pařez, G.C. Gabriela, H. Hasse, J. Vrabe, Mutual diffusion in the ternary mixture of water + methanol + ethanol and its binary subsystems, Phys. Chem. Chem. Phys. 15 (2013) 3985–4001.
[14] G. D'Errico, G. Mangiapia, O. Ortona, Mutual and intradiffusion coefficients for the binary system *n*-decyl dimethyl phosphine oxide + water at 25 °C, J. Chem. Eng. Data 53 (2008) 1651–1654.
[15] D.G. Leaist, L. Hao, Simultaneous measurement of mutual diffusion and intradiffusion by taylor dispersion, J. Phys. Chem. 98 (1994) 4702–4706.
[16] V.C.P. da Costa, A.C.F. Ribeiro, A.J.F.N. Sobral, V.M.M. Lobo, O. Annunziata, C.I.A. V. Santos, S.A. Willis, W.S. Price, M.A. Esteso, Mutual and self-diffusion of charged porphyrines in aqueous solutions, J. Chem. Thermodyn. 47 (2012) 312–319.
[17] A. Plugatyr, I.M. Svishchev, Molecular diffusivity of phenol in sub- and supercritical water: application of the split-flow Taylor dispersion technique, J. Phys. Chem. B 115 (2011) 2555–2562.
[18] J. Wang, T. Hou, Application of molecular dynamics simulations in molecular property prediction II: diffusion coefficient, J. Comput. Chem. 32 (2011) 3505–3519.
[19] X. Tang, P.H. Koenig, R.G. Larson, Molecular dynamics simulations of sodium dodecyl sulfate micelles in water—the effect of the force field, J. Phys. Chem. B 118 (2014) 3864–3880.
[20] J.M.P.Q. Delgado, Molecular diffusion coefficients of organic compounds in water at different temperatures, J. Phase Equilib. Diffus. 28 (2007) 427–432.
[21] M. Fioroni, M.D. Diaz, K. Burger, S. Berger, Solvation phenomena of a tetrapeptide in water/trifluoroethanol and water/ethanol mixtures: a diffusion NMR, intermolecular NOE and molecular dynamics study, J. Am. Chem. Soc. 124 (2002) 7737–7744.
[22] S. Paul, G.N. Patey, Influence of urea on *tert*-butyl alcohol aggregation in aqueous solutions, J. Phys. Chem. B 116 (2012) 4991–5001.
[23] I. Shvab, R.J. Sadus, Thermodynamic properties and diffusion of water + methane binary mixtures, J. Chem. Phys. 140 (2014) 104505.
[24] W.L. Jorgensen, D.S. Maxwell, T.-R. Julian, Development and testing of the OPLS all-atom force field on conformational energetics and properties of organic liquids, J. Am. Chem. Soc. 118 (1996) 11225–11236.
[25] P. Mark, L. Nilsson, Structure and dynamics of the TIP3P, SPC, and SPC/E water models at 298 K, J. Phys. Chem. A 105 (2001) 9954–9960.
[26] C. Zhang, X. Yang, Molecular dynamics simulation of ethanol/water mixtures for structure and diffusion properties, Fluid Phase Equilib. 231 (2005) 1–10.
[27] S. Nose, A molecular dynamics method for simulations in the canonical ensemble, Mol. Phys. 52 (1984) 255–268.
[28] M. Parrinello, A. Rahman, Polymorphic transitions in single crystals: a new molecular dynamics method, J. Appl. Phys. 52 (1981) 7182–7190.
[29] P. Edwald, The calculation of optical and electrostatic grid potential, Ann. Phys. 1965 (1921) 2732–2737.
[30] K. Yui, N. Yamazaki, T. Funazukuri, Infinite dilution binary diffusion coefficients for compounds derived from biomass in water at 0.1 MPa and temperatures from (298.2 to 353.2) K, J. Chem. Eng. Data 58 (2013) 183–186.
[31] D. Frenkel, B. Smit, Understanding Molecular Simulation, Academic Press, United States of America, 1996.
[32] I.G. Economou, N.M. Garrido, Z.A. Makrodimitri, Prediction of microscopic structure and physical properties of complex fluid mixtures based on molecular simulation, Fluid Phase Equilib. 296 (296) (2010) 125–132.
[33] E. Matteoli, G.A. Mansoori, A simple expression for radial distribution functions of pure fluids and mixtures, J. Chem. Phys. 103 (1995) 4672–4677.
[34] D. Montgomery, Design and Analysis of Experiments, Willey, London, 2009.
[35] Y. Wang, B. Abrahamsson, L. Lindfors, J.G. Brasseur, Comparison and analysis of theoretical models for diffusion-controlled dissolution, Mol. Pharm. 9 (2012) 1052–1066.
[36] P.K. Srinivasa, R. Varanasi, S. Yashonath, Dependence of diffusivity on density and solute diameter in liquid phase: a molecular dynamics study of Lennard–Jones system, J. Chem. Phys. 136 (2012) 144505.
[37] I. Poudyal, N.P. Adhikari, Temperature dependence of diffusion coefficient of carbon monoxide in water: a molecular dynamics study, J. Mol. Liq. 194 (2014) 77–84.
[38] E. Karacabey, L. Bayindirli, N. Artik, G. Mazza, Modeling solid–liquid extraction kinetics of trans-resveratrol and *trans*-ε-viniferin from grape cane, J. Food Process Eng. 36 (2013) 103–112.
[39] L.F.G. Martins, M.C.B. Parreira, J.P.P. Ramalho, P. Morgado, E.J.M. Filipe, Prediction of diffusion coefficients of chlorophenols in water by computer simulation, Fluid Phase Equilib. 396 (2015) 9–19.
[40] M.N. Islam, Y.-T. Jo, S.-K. Jung, J.-H. Park, Thermodynamic and kinetic study for subcritical water extraction of PAHs, J. Ind. Eng. Chem. 19 (2013) 129–136.
[41] A.G. Carr, R. Mammucari, N.R. Foster, A review of subcritical water as a solvent and its utilisation for the processing of hydrophobic organic compounds, Chem. Eng. J. 172 (2011) 1–17.
[42] B.E. Poling, J.M. Prausnitz, J.P. O'Connell, The Properties of Gases and Liquids, McGraw-Hill, United States of America, 2001.
[43] K. Miyabe, R. Isogai, Estimation of molecular diffusivity in liquid phase systems by the Wilke–Chang equation, J. Chromatogr. A 1218 (2011) 6639–6645.
[44] T. Funazukuri, C.Y. Kong, S. Kagei, Binary diffusion coefficients in supercritical fluids: recent progress in measurements and correlations for binary diffusion coefficients, J. Supercrit. Fluids 38 (2006) 201–210.
[45] M. Tanaka, Y. Takahashi, N. Yamaguchi, K.-W. Kim, G. Zheng, M. Sakamitsu, The difference of diffusion coefficients in water for arsenic compounds at various pH and its dominant factors implied by molecular simulations, Geochim. Cosmochim. Acta 105 (2013) 360–371.
[46] H. Ueno, M. Tanaka, M. Hosino, M. Sasaki, M. Goto, Extraction of valuable compounds from the flavedo of *Citrus junos* using subcriticalwater, Sep. Purif. Technol. 62 (2008) 512–516.
[47] J.D. Espinoza-Pérez, A. Vargas, V.J. Robles-Olvera, G.C. Rodríguez-Jimenes, M.A. García-Alvarado, Mathematical modeling of caffeine kinetic during solid–liquid extraction of coffee beans, J. Food Eng. 81 (2007) 72–78.
[48] J. Hu, Z. Guo, M. Glasius, K. Kristensen, L. Xiao, X. Xu, Pressurized liquid extraction of ginger (*Zingiber officinale* Roscoe) with bioethanol: an efficient and sustainable approach, J. Chromatogr. A 1218 (2011) 5765–5773.